Int. J. Heat Mass Transfer. Vol. 16, pp. 411–425. Pergamon Press 1973. Printed in Great Britain

DROPWISE CONDENSATION—THE DISTRIBUTION OF DROP SIZES

J. W. ROSE
Department of Mechanical Engineering, Queen Mary College, University of London, England

and

L. R. GLICKSMAN
Department of Mechanical Engineering, Massachusetts Institute of Technology, Cambridge, Mass., U.S.A.

(*Received* 21 *February* 1972 *and in revised form* 12 *June* 1972)

Abstract—The nature of the drop growth process during dropwise condensation, as revealed by high magnification cine films [16–18, 29], is used as the basis of a simplified model of the sequence of events occurring during the growth cycle (i.e. the time interval between successive sweepings of the region of the surface under consideration). The model is used to predict the average distribution of drop sizes. The theoretical distribution is compared with measurements [8, 31], a recent computer simulation [32] and an earlier empirical distribution [28].

NOMENCLATURE

$A(r)$, distribution function;
a, radius of circles in uniform array (see Fig. 3);
f, fraction of available area covered by a generation of drops;
$N(r)$, distribution function;
n_i, number of drops of generation i per area;
m, largest integer for which $\gamma^m \geqslant r/\hat{r}_0$;
p, defined in equation (17);
q, defined in equation (18);
r, radius;
$\hat{r}_i$, maximum radius of drops of generation i;
r_u, upper radius of range;
r_l, lower radius of range;
S, volume of a drop divided by cube of the base radius;
s, distance between centres of neighbouring circles in uniform array (see Fig. 3);
t, time;
V, total volume condensation rate per area.

Greek letters

α, fraction of total area covered by all drops having radii greater than r;
γ, $\hat{r}_{i+1}/r_i$ when generation $i+1$ has radius $\hat{r}_{i+1}$;
Δr, $r_u - r_l$;
τ, time interval between cycles of generation 0;
ψ, defined in equation (20).

Subscripts—0, 1, 2 ... i denote particular generations of drops.

1. INTRODUCTION

SINCE Schmidt *et al.* [1] reported their discovery of a second "ideal" mode of condensation, i.e. dropwise condensation, and the fact that, for steam, the vapour-side heat-transfer coefficient was much higher than that for the filmwise mode, considerable effort has been directed toward understanding the mechanism of dropwise condensation. Only relatively recently, however, have many of the apparent discrep-

ancies between the experimental results of different workers, and conflicting opinions regarding various aspects of the mechanism, been settled.

There is now considerable evidence to support the following:

(a) When the effects of non-condensing gas are eliminated,* the vapour-side coefficient for both steam [2–9] and mercury [10] increases with heat flux and is not strongly dependent on vapour velocity [6, 8, 11].
(b) Promoter used and surface roughness have small but measurable effect on the vapour-side coefficient [3–5, 8].
(c) Surface inclination has relatively small effect on the vapour-side coefficient except for large deviations from the vertical [2, 12–14].
(d) Condensation on newly exposed areas is in the form of minute drops and condensate films greater than monomolecular thickness are not present [15–18].

While progress has been made in recent years towards understanding the mechanism of dropwise condensation, there still remain areas of uncertainty. The problem is complicated by the existence on the condensing surface of a very wide range of drop sizes, extending from the "primary" drops (those which form at nucleation sites and grow by condensation) to the largest which can remain on the surface, the latter drops being several orders of magnitude larger than the former. Several factors are involved in the mechanism of heat transfer during dropwise condensation, their relative significance depending on the drop size. Thus for the smallest drops the effect of surface curvature on the saturation temperature and pressure is of major importance while for larger drops conduction is the dominating factor. Since the condensation rate on small drops of near-to-optimum size can be very large (much larger than that averaged over the whole condensing surface), the resistance associated with interphase matter transfer [19] plays an important role in the case of these drops. In addition, a further resistance, associated with non-uniformities of heat flux in the material of the condenser wall near to the condensing surface, has been proposed [20]. Recent work on yet another factor of possible importance, i.e. that of thermocapillary convection within the drops [21], suggests that this effect is of minor significance.

While considerable progress has been made on the problem of calculating the heat transfer through a single drop of given size, the problem of the distribution of drop sizes is less well understood. In attempting to calculate the average heat-transfer rate, different workers have dealt with the problem of the drop size distribution in a variety of ways. Fatica and Katz [22] and Sugawara and Michiyoshi [23] assumed that on a given area all drops have the same size, are uniformly spaced and grow by condensation at their surfaces. Wenzel [24] assumed that drops grow in uniform square array and that coalescences occur between four neighbouring drops to form a larger drop in a new uniform square array. Gose, Mucciardi and Baer [25] and more recently, Tanasawa and Tachibana [26] have attempted partially to model the drop growth and coalescence process by computer. The major problem here was the large time requirement to model the process adequately. (This is illustrated by reports of nucleation site density 2×10^6 sites/mm^2 [8] and that about 400 000 coalescences may be involved in the formation of a single drop of radius about 1 mm [27].) Le Fevre and Rose [28] assumed a form for the distribution function which had the correct behaviour for the limiting cases of very large and very small drops.

All of the above treatments are either incomplete or at variance with the evidence provided by the high magnification cine films of Westwater and co-workers [16–18, 29]. This photographic evidence forms the basis of the present model of drop growth and coalescence.

* Minute traces of non-condensing gases such as remain after prolonged boiling have a significant effect on the steam-side coefficient [4].

2. DESCRIPTION OF THE CONDENSATION PROCESS

A photograph of dropwise condensation on a plane vertical surface, covering a region containing several of the largest size drops but excluding falling drops, shows that the largest drops are all much the same size and are more or less uniformly spaced. Other drops are considerably smaller. An enlarged photograph of a region between the largest drops (covering as large an area as possible without including the largest drops) appears virtually identical to the former picture; i.e. the largest drops on the photograph are approximately uniform in size and spacing, other drops being a good deal smaller. The same is true again of the region between the largest drops on the above picture, and so on.

Alternatively, one may follow the sequence of events on a region of the condensing surface between successive sweepings. Primary drops are first formed at nucleation sites. These grow by condensation until coalescence occurs between neighbours. The coalesced drops continue to grow and new ones to form and grow at sites exposed through coalescence. As the process continues, coalescences occur between drops of various sizes while the size of the largest drops present continues to increase. A situation is soon reached where the largest drops present appear more or less uniform in size and spacing. This situation persists as these largest drops grow and their number per area decreases until they reach a size at which the region is again swept. Of course, we cannot obtain a picture of sufficient size and resolution to follow the process through the entire cycle. What one in fact sees, when observing a small region under a microscope, is that the largest drops, by growing and in turn coalescing with neighbours become more widely spaced and pass out of the field of view.* When this occurs a second generation of "largest" drops, apparently indistinguishable from the earlier generation, may be recognised. These again grow and pass out of the field of view to be followed by a third generation and so on until a falling drop sweeps the entire field and the process restarts.

The important features of the above description of the condensation process are:

(a) the existence of distinct "generations" of drops.
(b) the fact that the drops of any generation are more or less uniform in size and spacing.
(c) the density of packing of a given generation on the available area (area not covered by larger drops), is apparently independent of the size of the drops and the same for all generations.

The explanation of the features described above lies primarily in the fact that, apart from those drops which are so small that the effect of interface curvature is significant, the time rate of increase in radius becomes smaller as the radius increases. For growth by direct condensation this can be seen from equation (14) of [28]. For growth by coalescence with other drops, we might expect the rate at which a drop increased its volume by capturing neighbours to be a function of its perimeter. If volume growth rate of a drop were proportional to its perimeter, then the rate of increase in its radius would vary inversely as the radius. The fact that the smaller drops of a generation grow more rapidly than the larger ones, tends to preserve uniformity of size.

Where drops of a given generation chance to be more closely packed, coalescence between neighbours tends to increase the spacing. Where drops of a given generation chance to be more widely spaced, fewer coalescences occur as these drops grow and consequently they become more closely packed. Occasionally, in a sparsely populated (by a given generation) region, the more rapid growth and coalescence of smaller drops (not of the generation under consideration) might provide a new member of the generation. Each of the above-mentioned fac-

* Occasionally one of the largest drops obscures the whole field for a time.

tors contributes towards a tendency to preserve uniformity of spacing.

3. THE PRESENT MODEL

A complete growth cycle is the time between successive sweepings of the region under consideration. Let us consider a somewhat idealized picture of the sequence of events during this time interval. The initial generation nucleates, the drops of this generation proceed to grow in size, while their number decreases through coalescences, until the region is reswept. The growth of the initial generation is illustrated in Fig. 1. The "typical" radius (drops of a real generation vary somewhat in size) at any instant is r_0 and its maximum value, i.e. at the end of the growth cycle of period τ, is $\hat{r}_0$. In Fig. 1, the

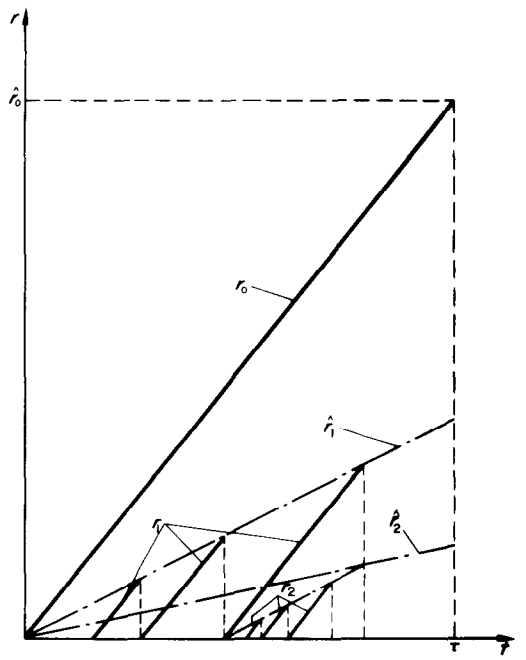

FIG. 1. Typical growth cycles for the first three generations of drops.

variation of r_0 with time is shown as a straight line through the origin. Real drops do not start with zero radius and some time may elapse, following sweeping, before the initial generation is formed. Furthermore there is at this stage no reason to suppose that r_0 should vary linearly with time. These matters are not relevant to the discussion at this stage, though it may be pointed out here that linear growth of r_0 does not imply that the radii of individual drops increase linearly, since the number of drops in the generation also varies with time.

During the growth of the generation, the balance between growth of individual drops and decrease in their numbers through coalescences, leads to a constant "size-to-spacing" ratio, i.e. as the drops grow larger they become proportionally more widely spaced. (This may be seen by enlarging a photograph, taken at an early stage in the growth of a generation, so that the typical radius is the same size as that in a photograph taken at a later stage. The two pictures are virtually indistinguishable.)

After some time interval from the start of the growth cycle, the next generation nucleates and commences to grow (in the space between the drops of the initial generation) in the same manner as its predecessor, i.e. the typical radius r_1 follows a path parallel to that of r_0. As time proceeds the ratio r_1/r_0 increases and consequently the ratio of the mean spacing of generation 1 to that of generation 0 increases. Thus drops of generation 1 are progressively captured by (i.e. coalesce with) drops of generation 0, until finally no drops of generation 1 remain. At this time another set of generation 1 drops is born and, by spreading, again feeds the drops of generation 0 until it again is entirely lost in the initial generation. Generation 1 disappears for the second time when the ratio of its spacing to that of generation 0, is the same as that at the end of the previous growth cycle of generation 1, i.e. at the same value of r_1/r_0. Thus the peak values of r_1 lie along the straight line $\hat{r}_1$. Three typical cycles of generation 1 are shown in Fig. 1.

In a similar manner, drops of generation 2, having a radius at any instant r_2, grow in the space between the drops of generation 1 and are captured by the latter. In Fig. 1, three typical growth cycles of generation 2 are shown in one of

the cycles of generation 1. Similarly, generation 3 forms and grows between drops of generation 2 and so on.

The following points may be noted in the above model of drop growth:

(1) the fraction of "available area", f, covered by drops of any generation is constant. By available area is meant area between the larger drops of older generations.
(2) the ratio, γ, of the maximum radius of any generation $\hat{r}_{i+1}$, to the radius of its immediate predecessor, r_i, at the instant when the former (i.e. generation $i + 1$) reaches its maximum value, is constant.

In order to determine the average distribution of drop sizes over a complete cycle (i.e. a growth cycle of generation 0), we require values of f and γ as well as growth rate of a generation as function of time.

Determination of f

The stable configuration of a generation (i.e. constant ratio between drop radius and mean spacing and hence constant f) arises from a balance between packing, due to growth of individual drops, and spacing, due to coalescence. In the real situation f is not of course strictly constant but fluctuates about some mean value.

In order to determine f, a computer programme was devised to model the growth of a generation. Starting from an initial configuration of non-overlapping circles in a plane, the radii of these circles were increased one by one, such that the smaller the radius, the greater its fractional increase. Various starting configurations and growth-rate functions were used.

After the radius of each circle was increased, a check was made for "coalescence". If the enlarged circle overlapped another circle, its radius was first set to the value at which the two circles just touched; the two were then coalesced, i.e. a single larger circle replacing the two former ones. For this purpose the circles were treated as representing drops which were segments of spheres (hemispheres or smaller), the volume of the new drop being set equal to the sum of the volumes of drops before coalescence and the position of the new drop being set at the centre of mass of the former pair. Checks for subsidiary coalescence were then made to determine whether, as a result of the coalescence, the new larger drop overlapped others. If this was the case, further coalescences were made in the manner described above except that in this case the radius was not set to the value at which the circles just touched before carrying out the coalescence. Again checks for further subsidiary coalescences were made until the remaining circle overlapped no others. The radius of the next circle was then increased and the process repeated.

In calculating the total area covered by all of the circles at any time, checks were made to determine whether or not each circle lay wholly in the field (i.e. the circular region containing the centres of all of the circles of the initial configuration). Where circles lay partly outside the field, only that portion inside was used to determine f, the total area covered by all of the circles divided by the area of the field.

Three starting configurations were used:

(1) 200 randomly spaced small circles having the same radius. The initial area covered by circles was 0·005.
(2) 200 randomly spaced circles having random radii (with maximum-to-minimum radius ratio of 1000). The initial area covered by circles was 0·34.
(3) 361 circles in close-packed (almost touching) uniform triangular array. The initial area covered by circles was 0·88.

In the above the area of the field was unity. In (1) the locations were determined by using random numbers as were the locations and radii in (2). In choosing these parameters to set up the initial configuration, circles which overlapped previously chosen circles were discarded.

Three different growth functions or size increments were used, corresponding to rates of

increase in radius proportional to radius to the powers: -0.5, -1 and -2.

It was found that whatever starting configuration or growth function was used, as the process progresses, the configuration evolves into that exhibited by the real generations of drops as seen in the films of Westwater *et al.* [16–18, 29]. Thus, as the number of circles becomes smaller, their radii and spacing become uniform. After the initial transient period, the value of f "settles down" to a value close to 0·55, occasionally falling as low as 0·48 when several "drops" are involved in a multiple coalescence or when several coalescences occur in close succession, and occasionally rising to about 0·62 when the circles chance to be more uniformly spaced and can grow appreciably without coalescing. The number of circles remaining when f reached its "steady" value was about 40 when using starting configuration (1) and about 70 when using starting configuration (2). When using starting configuration (3), f was equal to 0·51 after a single "round" of radius increases and the number of circles remaining was 64. For any starting configuration, when a few drops only remained, the fluctuations in f tended to be more violent but around the same mean, so that an average of the results from the later stages of several runs was close to 0·55.

Figure 2 shows the appearance during the later stages of the simulated growth of a generation. The lower figure shows the situation a short time after that of the upper figure. It can be seen that a group of four drops, as well as a pair, have each coalesced to form single drops reducing the total number from 13 to 9.

Earlier a simpler model had been used to provide an estimate for f. The foregoing description of the growth of a generation indicates that, at any instant, the drops are all of similar size and the density of packing is limited by coalescence between neighbours. It was considered that the instantaneous appearance of a generation might approximate to that of "maximum packing" of circles having equal radii and random locations with the restriction that no circles overlap. An experiment was carried out by computer to determine the value of f for such a situation. The centres of circles having radii 0·1 were chosen at random in a circular field of radius unity. Circles were rejected when they overlapped previously chosen circles. The fraction of the area of the field covered when no further circles could be accommodated gave an estimate of f. Several runs were carried out giving values of f in the range 0·5–0·56.

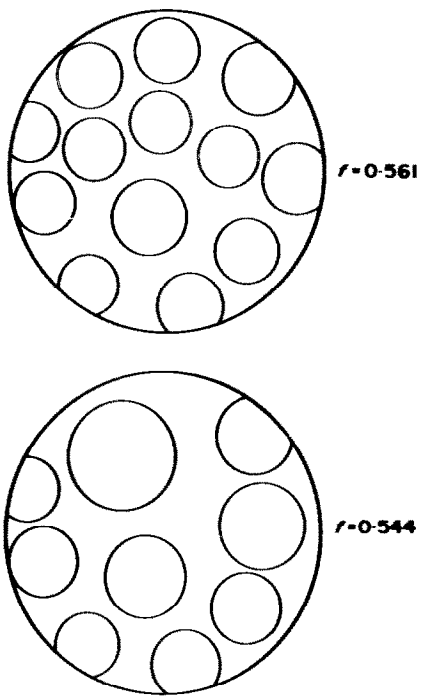

FIG. 2. Appearance of later stages in simulated growth of a generation.

Values of f were also found by measurement. Several frames of the Westwater films, selected from different stages of the growth cycle (i.e. larger or smaller numbers of drops per area) of different generations, were projected on to a screen and the image traced. By measurement of the tracings the following values of f were obtained: 0·51, 0·48, 0·51, 0·59, 0·57.

It may thus be concluded that the correct value of f lies in the range 0·5–0·6 and is probably close to 0·55.

Determination of γ

In order to estimate this parameter we idealize an actual generation, in which the drops have approximately the same size and approximately uniform spacing, to one in which the drops have identical sizes and are uniformly spaced i.e. their centres form an equilateral triangular array. Figure 3a shows three drops of such an ideal generation having, at some instant, radius a and distance between centres of neighbouring drops s. At this instant, the maximum radius which can be attained by a drop of the succeeding generation is equal to the distance between its centre and the perimeter of the nearest drop of the older generation. The maximum radius of a drop whose centre is at P is x (see Fig. 3a). We estimate the average value of the maximum radius which the newer generation could attain at the instant depicted in Fig. 3a as the average value of x given that P has equal probability of lying anywhere in the space between the drops of the older generation. Thus the average value of the maximum attainable radius, $\bar{x}$, is given by:

$$\bar{x} = \frac{1}{X}\iint_X x \, dX \tag{1}$$

where X is the area between the drops of the older generation. Then, referring to Fig. 3b

$$\bar{x} = \frac{\int_0^{\pi/6}\int_a^{s/2\cos\theta} (r-a)r \, dr \, d\theta}{\int_0^{\pi/6}\int_a^{s/2\cos\theta} r \, dr \, d\theta}. \tag{2}$$

Evaluating the above we find:

$$\gamma = \frac{\bar{x}}{a} = \frac{\frac{1}{24}\left(\frac{1}{3}+\frac{1}{4}\ln 3\right) - \frac{1}{8\sqrt{3}}\left(\frac{a}{s}\right) + \frac{\pi}{36}\left(\frac{a}{s}\right)^3}{\frac{1}{8\sqrt{3}}\left(\frac{a}{s}\right) - \frac{\pi}{12}\left(\frac{a}{s}\right)^3}. \tag{3}$$

Now for a uniform equilateral triangular array, the fractional area covered f is given by:

$$f = \frac{2\pi}{\sqrt{3}}\left(\frac{a}{s}\right)^2. \tag{4}$$

From equations (3) and (4), we find, for $f = 0{\cdot}5$, $0{\cdot}55$ and $0{\cdot}6$, the corresponding values $0{\cdot}224$, $0{\cdot}189$ and $0{\cdot}158$ respectively for γ.

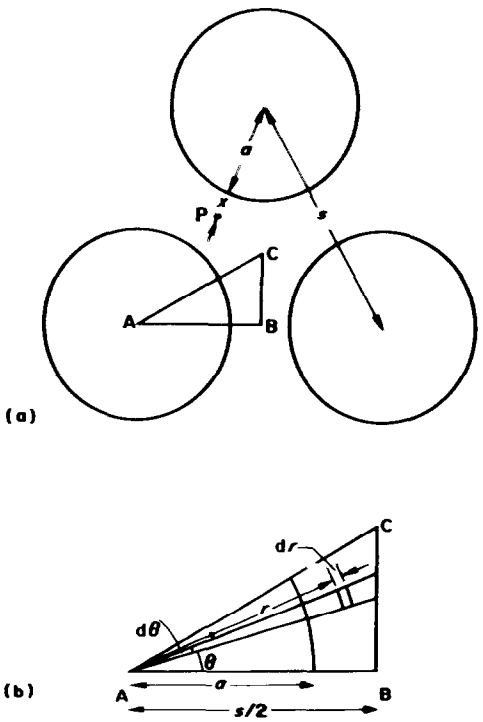

FIG. 3. Determination of γ.

Growth rate of a generation

The individual drops of a generation grow by: (a) direct condensation at their surface, (b) capture of succeeding generations and (c) coalescences between neighbouring drops of the same generation. A detailed analysis would thus be extremely involved and would include, through (a), all of those factors which are concerned in the heat-transfer to and through a single drop (see for instance [28]). However, since growth by direct condensation is only significant for very small drops* we shall proceed more simply

* This may not be true for a liquid such as mercury with high thermal conductivity.

and bear in mind the fact that our result may not be valid for very small drops.

Since each generation occupies a constant fraction of the total area irrespective of the stage of its development, the area available for the later generations of drops, which undergo many cycles and only achieve a very small maximum radius, remains constant. Since most of the condensation takes place on these small drops, we might expect that the total condensation rate would remain approximately constant with time. This conclusion is supported by heat-transfer measurements at different heights on vertical plates [3, 4] and using different surface inclinations [2, 12–14]. In both cases it has been found that for ranges over which the sweeping frequency varies appreciably,* the heat-transfer rate varied by a small or undetectable amount.

Thus, if we assume that the total volume condensation rate per area V is constant we have:

$$V = \frac{\mathrm{d}}{\mathrm{d}t} \Sigma (n_i S r_i^3) = \text{constant} \tag{5}$$

where the summation is taken over all generations. n_i is the number of drops per area of generation i and S is a shape factor equal to the volume of a drop divided by the cube of the radius, i.e. S is a constant for similar drops. Now

$$n_i = \frac{f(1-f)^i}{\pi r_i^2} \tag{6}$$

thus

$$V = \frac{Sf}{\pi} \frac{\mathrm{d}}{\mathrm{d}t} \Sigma \{r_i (1-f)^i\}. \tag{7}$$

Since the growth rate depends only on radius, i.e. is the same for all generations when at any given radius, we have, for any generation:

$$\frac{\mathrm{d}r_i}{\mathrm{d}t} = \phi(r).$$

Then, for constant V, from equation (7)

$$\sum (1-f)^i \frac{\mathrm{d}r_i}{\mathrm{d}t} = \Sigma (1-f)^i \phi(r) = \text{constant}. \tag{8}$$

Since equation (8) must hold when different generations are at various stages of growth and since the relationship between r_i and r_{i+1} is not fixed, the only solution which will hold in general is that $\phi(r)$ is a constant for all r and i. Thus the growth curves would be straight parallel lines as shown in Fig. 1.

4. DISTRIBUTION OF DROP SIZES

To determine $N_i(r)\,\mathrm{d}r$, the average number of drops per area of generation i in the size range r, $r + \mathrm{d}r$, we multiply n_i by the fraction of the cycle time τ which the drops spend in this size range, i.e.

$$N_i(r)\,\mathrm{d}r = n_i\,\mathrm{d}t_i/\tau. \tag{9}$$

Thus for generation 0:

number of drops per area of radius r, $n_0 = \dfrac{f}{\pi r^2}$

fraction of cycle time in size range r, $r + \mathrm{d}r$

$$= \frac{\mathrm{d}t_0}{\tau} = \frac{\mathrm{d}r}{\hat{r}_0}$$

hence:

$$N_0(r)\,\mathrm{d}r = \frac{f}{\pi r^2} \frac{\mathrm{d}r}{\hat{r}_0} \qquad (r \leqslant \hat{r}_0). \tag{10}$$

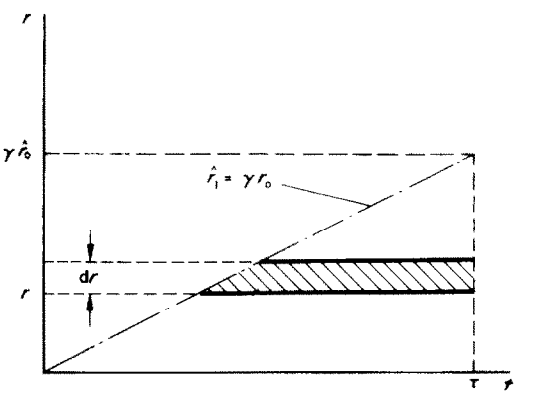

FIG. 4. Estimation of time spent by generation 1 in size range r, $r + \mathrm{d}r$.

* Sweeping frequency increases: (1) with distances from the top of the surface since a falling drop grows, and hence sweeps a diverging path, and (2) with inclination since the size at which a drop begins to fall, and its speed of descent, depend on the surface inclination.

Turning now to generation 1, the growth cycles shown in Fig. 1 do not have a definite location on the time axis. Here we shall assume that all locations are equally probable, i.e. for drops of generation 1, at any instant, there is equal probability that the radius lies between zero and its maximum possible value at that instant. This will also be assumed for all subsequent generations. On this basis, referring to Fig. 4 we estimate the fraction of the cycle time τ, spent by drops of generation 1 in the size range $r, r + \mathrm{d}r$ ($r \leqslant \gamma \hat{r}_0$), as the ratio of the area of the shaded strip to the total area under $\hat{r}_1$, thus:

$$\frac{\mathrm{d}t_1}{\tau} = \frac{\left(1 - \frac{1}{\gamma}\frac{r}{\hat{r}_0}\right)\tau\,\mathrm{d}r}{\frac{1}{2}\gamma\tau\hat{r}_0}$$

$$= \frac{2}{\gamma}\left(1 - \frac{1}{\gamma}\frac{r}{\hat{r}_0}\right)\frac{\mathrm{d}r}{\hat{r}_0} \qquad (r \leqslant \gamma\hat{r}_0) \quad (11)$$

and, in general, for generation i $(i \geqslant 1)$;

$$\frac{\mathrm{d}t_i}{\tau} = \frac{\left(1 - \frac{1}{\gamma^i}\frac{r}{\hat{r}_0}\right)\tau\,\mathrm{d}r}{\frac{1}{2}\gamma^i\tau\hat{r}_0}$$

$$= \frac{2}{\gamma^i}\left(1 - \frac{1}{\gamma^i}\frac{r}{\hat{r}_0}\right)\frac{\mathrm{d}r}{\hat{r}_0}\,3 \qquad (i \geqslant 1, r \leqslant \gamma^i\hat{r}_0) \quad (12)$$

then, using equations (6) and (9) we have:

$$N_i(r)\,\mathrm{d}r = \frac{f(1-f)^i}{\pi r^2}\frac{2}{\gamma^i}\left(1 - \frac{1}{\gamma^i}\frac{r}{\hat{r}_0}\right)\frac{\mathrm{d}r}{\hat{r}_0}$$

$$(i \geqslant 1, r \leqslant \gamma^i\hat{r}_0). \qquad (13)$$

Thus, accounting for all generations whose maximum attainable radius, $\gamma^i\hat{r}_0$ exceeds r we obtain the required distribution of drop sizes:

$$N(r)\,\mathrm{d}r = N_0(r)\,\mathrm{d}r + \sum_{i=1}^{m} N_i(r)\,\mathrm{d}r \qquad (14)$$

where m is the largest integer for which $\gamma^m \geqslant r/\hat{r}_0$ i.e. m = entier $\{\ln(r/\hat{r}_0)/\ln\gamma\}$ (higher generations, $i > m$, do not contribute since their maximum attainable radius is less than r). Thus:

$$N(r)\,\mathrm{d}r = \frac{f}{\pi\hat{r}_0}\left[1 + 2\sum_{i=1}^{m}\left\{\frac{(1-f)^i}{\gamma^i} \times \left(1 - \frac{1}{\gamma^i}\frac{r}{\hat{r}_0}\right)\right\}\right]\frac{\mathrm{d}r}{r^2}. \qquad (15)$$

For the purpose of calculating the average heat flux the fractional area $A(r)\,\mathrm{d}r$ covered by drops in the size range r, $r + \mathrm{d}r$ is required. This is given immediately by multiplying equation (15) by πr^2:

$$A(r)\,\mathrm{d}r = \frac{f}{\hat{r}_0}\left[1 + 2\sum_{i=1}^{m}\left\{\frac{(1-f)^i}{\gamma^i} \times \left(1 - \frac{1}{\gamma^i}\frac{r}{\hat{r}_0}\right)\right\}\right]\mathrm{d}r. \qquad (16)$$

When integrating equations (15) or (16) to obtain precise results for a finite size range, it is necessary to distinguish those generations for which the upper limit of integration is the upper radius of the range and those whose maximum attainable radius may be less than the upper limit of the range. Thus, in order to calculate the number of drops per area having radii between upper and lower bounds respectively of r_u and r_1 we have, for generations 0 to p an upper limit of integration r_u and for generations $p + 1$ to q and upper limit of $\gamma^i\hat{r}_0$, i denoting the generation in question, and

$$p = \text{entier}\,\{\ln(r_u/\hat{r}_0)/\ln\gamma\} \qquad (17)$$

$$q = \text{entier}\,\{\ln(r_1/\hat{r}_0)/\ln\gamma\}. \qquad (18)$$

Equation (15) may be written:

$$N(r)\,\mathrm{d}r = \frac{f}{\pi\hat{r}_0}\left\{1 + 2\sum_{i=1}^{p}\psi(i,r) + 2\sum_{i=p+1}^{q}\psi(i,r)\right\}\frac{\mathrm{d}r}{r^2} \qquad (19)$$

where

$$\psi(i,r) = \frac{(1-f)^i}{\gamma^i}\left(1 - \frac{1}{\gamma^i}\frac{r}{\hat{r}_0}\right). \qquad (20)$$

The number of drops per area in the size range r_1, r_u is then given by:

$$N(r)\,\Delta r = \frac{f}{\pi \hat{r}_0}\left\{\int_{r_1}^{r_u}\frac{dr}{r^2} + 2\int_{r_1}^{r_u}\sum_{i=1}^{p}\frac{\psi(i,r)}{r^2}dr + 2\int_{r_1}^{\gamma^q \hat{r}_0}\sum_{i=p+1}^{q}\frac{\psi(i,r)}{r^2}dr\right\} \quad (21)$$

evaluating the integrals we have:

$$N(r)\,\Delta r = \frac{f}{\pi \hat{r}_0}\left\{\left(\frac{1}{r_1}-\frac{1}{r_u}\right) + 2\sum_{i=1}^{p}\frac{(1-f)^i}{\gamma^i}\left[\left(\frac{1}{r_1}-\frac{1}{r_u}\right)-\frac{1}{\gamma^i\hat{r}_0}\ln\left(\frac{r_u}{r_1}\right)\right] + 2\sum_{i=p+1}^{q}\frac{(1-f)^i}{\gamma^i}\left[\left(\frac{1}{r_1}-\frac{1}{\gamma^i\hat{r}_0}\right) - \frac{1}{\gamma^i r_0}\ln\left(\frac{\gamma^i\hat{r}_0}{r_1}\right)\right]\right\}. \quad (22)$$

Similarly for the fractional area covered by drops in the size range r_1, r_u, we find:

$$A(r)\,\Delta r = \frac{f}{\hat{r}_0}\left\{r_u - r_1 + 2\sum_{1}^{p}\frac{(1-f)^i}{\gamma^i}\times\left[r_u - r_1 - \frac{1}{2\gamma^i\hat{r}_0}(r_u^2 - r_1^2)\right] + 2\sum_{p+1}^{q}\frac{(1-f)^i}{\gamma^i}\left[\gamma^i\hat{r}_0 - r_1 - \frac{1}{2\gamma^i\hat{r}_0}\times(\gamma^{2i}\hat{r}_0^2 - r_1^2)\right]\right\}. \quad (23)$$

For the special case when $r_1 = r$ and $r_u = \hat{r}_0$, equation (23) gives α, the fractional area covered by all drops having radius greater than r. In this case $p = 0$, $q = m$ and equation (23) becomes:

$$\alpha = f\left(1-\frac{r}{\hat{r}_0}\right) + 2f\sum_{i=1}^{m}\left\{\left(\frac{1-f}{\gamma}\right)^i \times\left(\frac{\gamma^i}{2} - \frac{r}{\hat{r}_0} + \frac{\gamma^{-i}}{2}\frac{r^2}{\hat{r}_0^2}\right)\right\}. \quad (24)$$

5. COMPARISON WITH MEASUREMENTS

Before comparison with measurements can be made it is necessary to understand what is meant by $\hat{r}_0$ in the real situation. While a generation of drops is a physical reality, the drops of an actual generation, at a given instant, vary somewhat in size. In the present model, drops of a given generation, i, have identical radii, r_i. Thus r_i corresponds to an average radius of the actual generation. In particular, at the instant before the region under observation is swept, by a falling drop, $\hat{r}_0$ corresponds to the average radius of the oldest (i.e. largest) generation of drops.

It is apparent that $\hat{r}_0$ is smaller than the largest single drop immediately prior to sweeping. Moreover in practice, the interval between successive sweepings of a given region varies somewhat and hence the maximum size attained by the oldest generation also fluctuates from cycle to cycle. Thus to obtain a proper measurement of $\hat{r}_0$, it would be necessary to obtain a large number of photographs of the region, taken at different times (under steady conditions) immediately prior to sweeping. Such photographs could conveneintly be obtained by extracting the appropriate frames from a cinéfilm taken over a sufficiently long time interval. From each photograph the average radius of the largest generation could be measured and second average taken over all photographs.

Recently, detailed measurements of the distribution of drop sizes for dropwise condensation of steam have been made [8, 31]. Measurements were made for different vapour-to-surface temperature differences [31], pressures [8] and surface inclinations [31] and in both investigations all drops down to those having radii of about 5 μm were counted. Since these authors do not comment on the "generations" of drop growth they, not surprisingly, give no direct information from which $\hat{r}_0$ can be found. However, it is possible to make rough estimates of $\hat{r}_0$ from the measurements given. If the number of drops per area in a given size range is plotted against the mean radius for the range,

one might expect a fall in numbers of drops and a discontinuity when the mean radius reaches a value for which the upper radius limit of the range exceeds $\hat{r}_0$. In the ideal case there are no drops having radius exceeding $\hat{r}_0$, while in the real case one would anticipate fewer drops with radius exceeding $\hat{r}_0$ than would be found by extrapolating from the distribution for smaller drops. All of the observed distributions [8, 31] exhibit this behaviour and provide us with a means of estimating $\hat{r}_0$ for each set of observations.

For example, Fig. 5 shows a typical set of observations showing a discontinuity at a

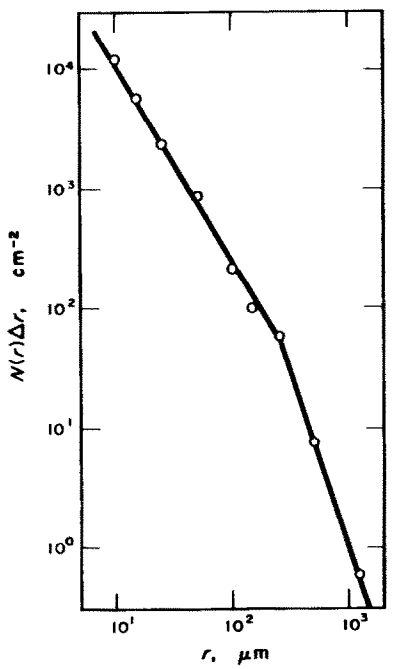

FIG. 5. Data of Graham [8] showing discontinuity at $r \simeq 0{\cdot}27$ mm. (Vertical surface, vapour temperature 100°C.)

radius of about 0·27 mm. This figure should perhaps be regarded as a lower bound since only two points (probably the least reliable) were used to construct the part of the curve to the right of the discontinuity. The size range used for counting was 0·8 r to 1·2 r, and hence we estimate the lower bound for $\hat{r}_0$ to be about 1·2 × 0·27 mm i.e. about 0·32 mm, with a less definite upper bound of about 0·4 mm. All of the data of Graham [8] and Tanasawa [31] were treated in this way and the estimated values of $\hat{r}_0$ are given (rounded to the nearest 0·05 mm) in the table below:—

Table 1

Author	Graham [8]		Tanasawa [31]		
Steam temperature, °C	100	31	100	100	100
Steam-to-surface temperature difference/K	0·28	0·28	1·0	2·0	1·3
Surface inclination/degree	90	90	90	90	45
$\hat{r}_0$/mm	0·35	0·45	0·35	0·6	0·35
Symbol Fig. 6	O	□	●	+	×

The variations in $\hat{r}_0$ with experimental conditions are not thought to be significant. It is considered more probable that these result from minor differences in surface properties following cleaning and promoting on separate occasions. This is supported by heat-transfer evidence [4], where measurements made on a particular occasion exhibited less scatter than found when comparing measurements made on separate occasions after cleaning and re-promoting. While, on the grounds of dimensional analysis [28], one might expect $\hat{r}_0$ to increase with decreasing temperature as indicated by the results of Graham, there is no reason to expect that for a vertical surface $\hat{r}_0$ should be greater for a somewhat greater condensation rate. The fact that $\hat{r}_0$ for a surface inclination of 45° was not found to be greater than for the vertical surface might at first seem surprising. However, heat-transfer measurements [2, 12–14] have shown that results are only weakly dependent on surface inclination for inclinations to the vertical of less than 60°.

In Fig. 6, the distribution function $N(r)$ (obtained from the measurements by dividing the number of drops per area in a given size

range by the range) is plotted against the geometric mean radius for the range. Those few points for which the upper limit of the radius range exceeded $\hat{r}_0$ have been omitted. It may be seen that the two sets of measurements are in good agreement and that no dependence on $\hat{r}_0$ can be discerned.

Included on Fig. 6 is the curve given by equation (15) using $f = 0{\cdot}55$, $\gamma = 0{\cdot}189$ and $\hat{r}_0 = 0{\cdot}45$ mm. $N(r)$ was also calculated using equation (22) and the size ranges used in the measurements. The differences between the results using equation (22) and those found from equation (15) were much smaller than the scatter of the measurements.

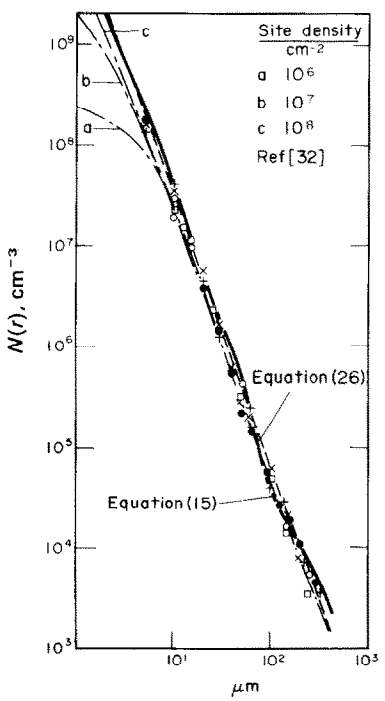

FIG. 6. Comparison of equations (15), (26) and computer simulations [32] with measured drop size distributions [8, 31]. (The symbols representing the measurements are identified in Table 1.)

The equation for the drop size distribution used by Le Fevre and Rose [28]:

$$\alpha = 1 - (r/\hat{r}_0)^{\frac{1}{3}} \tag{25}$$

gives:

$$N(r)\,dr = \frac{1}{3\pi r^2 \hat{r}_0}\left(\frac{r}{\hat{r}_0}\right)^{-\frac{2}{3}} dr. \tag{26}$$

Equation (26) is also shown in Fig. 6 using $\hat{r}_0 = 0{\cdot}45$ mm.

The results of a recent computer simulation of Glicksman and Hunt [32] is also included in Fig. 6.

It may be seen that equations (15) and (26) are in good agreement* with the measured distributions. The distributions found by Glicksman and Hunt, for different nucleation site densities merge with these results. Comparison of the Glicksman and Hunt distributions with the observations indicates that the nucleation site densities were, for the conditions under which the observations were made, at least 10^8 cm^{-2}.

Equation (15) may be safely used to calculate the heat transfer through drops of radius greater than about 5 μm. For simplicity in calculations, equation (15) can be closely approximated by a modified form of the earlier Le Fevre and Rose empirical distribution. The modified form is:

$$\alpha = 1 - (r/\hat{r}_0)^{0{\cdot}382}. \tag{27}$$

Figure 7(a) shows the effect of $\hat{r}_0$ on the distribution predicted by equation (15). The curves given are from equation (15) (with $f = 0{\cdot}55$, $\gamma = 0{\cdot}189$) using the smallest and largest estimates for $\hat{r}_0$ i.e. 0·35 mm and 0·6 mm. It may be seen that while the dependence of $N(r)$ on $\hat{r}_0$ in this range is not strong, the difference between the two curves for radii exceeding about 0·1 mm is greater than the scatter of the measurements.

It was mentioned earlier that while f was

* The distribution used by Le Fevre and Rose, equations (25) and (26) has earlier [33] been compared with the observations of Graham [8]. The fact that the agreement was less satisfactory than is here shown to be the case, was due to the fact that the radius of the largest visible drop had been used to non-dimensionalize the radius [34] rather than the effective maximum radius $\hat{r}_0$.

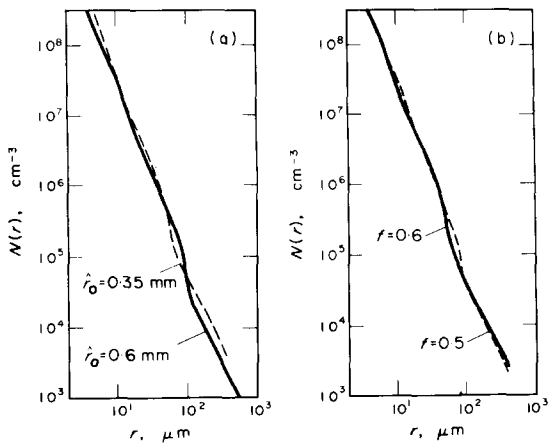

FIG. 7. The effects of $\hat{r}_0$ (with $f = 0{\cdot}55$, $\gamma = 0{\cdot}189$) and f (with $\hat{r}_0 = 0{\cdot}45$ mm) on the distribution of drop sizes given by equation (15).

estimated as 0·55 and thought to be close to the value, it was possible that f might be as low as 0·5 or as high as 0·6. The results obtained from equation (15) for the extreme values of f (using the corresponding values of γ and $\hat{r}_0 = 0{\cdot}45$ mm) are shown in Fig. 7(b). It may be seen that dependence of $N(r)$ on f in this range is smaller than the scatter of the measurements. Thus equally good agreement between theory on measurement would be obtained for all values of f in the range 0·5–0·6 (with the appropriate values of γ).

6. CONCLUDING REMARKS

The present description of the growth of a generation of drops (i.e. f remains constant as the average radius increases with time) does not hold for the primary drops which form at condensation sites and grow by direct condensation. Significant coalescence occurs when the average radius of the primary drops becomes equal to about half the mean spacing between the condensation sites. This value provides an absolute lower limit to the range of validity of the present model.

The theoretical distribution of drop sizes relates to a particular small region of the condensing surface. Since falling drops sweep diverging tracks, the lower regions of the surface are swept more frequently, and consequently $\hat{r}_0$ decreases with distance down the surface. (For a plane vertical surface of moderate height the frequency of sweeping varies approximately as the cube root of plate height [23].) In general, to determine the size distribution over a relatively large area, it would be necessary to determine the dependence of $\hat{r}_0$ on location and to integrate for the whole region. When considering larger areas it should also be noted that the theory does not include falling drops. (At the end of the growth cycle, the region under consideration is covered by a falling drop for a finite time which is ignored in the present analysis.) For water the fraction of surface area covered by falling drops is, except at very high condensation rates, small and may be taken account of separately [30].

The fact that the theory, which does not involve the vapour-to-surface temperature difference, vapour pressure and fluid properties i.e. the factors affecting the growth rate of individual drops, agrees well with measurements, suggests that, for the range of drop sizes covered by the measurements (5 μm radius and above), the coupling between the distribution of drop sizes and the heat-transfer parameters is weak. (For the conditions under which the measurements [8] were made the radius of the smallest viable drop is about 0·06 μm.)

Finally, it should be noted that the values of f and γ used in the present work are valid only for drops which are spherical segments having contact angles less than or equal to $\pi/2$. For drops having larger contact angles (e.g. mercury) coalescence occurs before the base radii come into contact. In the absence of any size distribution data for drops having contact angles significantly in excess of $\pi/2$ these cases have not been pursued at present.

REFERENCES

1. E. SCHMIDT, W. SCHURIG and W. SELLSCHOP, Versuche über die Kondensation von Wasserdampf un Film- und Tropfenform, *Tech. Mech. Thermo-Dyam., Berlin* **1**, 53 (1930).

2. H. WENZEL, Versuche über Tropfenkondensation. *Allg. Wärmetech.* **8**, 53 (1957).
3. E. J. LE FEVRE and J. W. ROSE, Heat-transfer measurements during dropwise condensation of steam. *Int. J. Heat Mass Transfer* **7**, 272 (1964).
4. E. J. LE FEVRE and J. W. ROSE, An experimental study of heat transfer by dropwise condensation. *Int. J. Heat Mass Transfer* **8**, 1117 (1965).
5. D. W. TANNER, C. J. POTTER, D. POPE and D. WEST, Heat transfer in dropwise condensation—Part I. *Int. J. Heat Mass Transfer* **8**, 419 (1965).
6. E. CITAKOGLU and J. W. ROSE, Dropwise condensation some factors influencing the validity of heat-transfer measurements. *Int. J. Heat Mass Transfer* **11**, 523 (1968).
7. D. W. TANNER, D. POPE, C. J. POTTER and D. WEST, Heat transfer in dropwise condensation at low steam pressures in the absence and presence of non-condensable gas. *Int. J. Heat Mass Transfer* **11**, 181 (1968).
8. C. GRAHAM, The limiting heat transfer mechanisms of dropwise condensation. Ph.D. Thesis, Mass. Inst. Tech. (1969).
9. R. WILMSHURST and J. W. ROSE, Dropwise condensation—further heat-transfer measurements. Proc. Fourth Int. Heat Transfer Conference **6**, paper Cs 1.4 (1970).
10. M. N. IVANOVSKII, V. I. SUBBOTIN and YU MILOVANOV, Heat transfer with dropwise condensation of mercury vapour. *Teploenergetika* **14** (6), 81 (1967).
11. D. W. TANNER, D. POPE, C. J. POTTER and D. WEST, Heat transfer in dropwise condensation—Part II. *Int. J. Heat Mass Transfer* **8**, 427 (1965).
12. H. HAMPSON and N. OZISIK, An investigation into the condensation of steam. *Proc. Instn Mech. Engrs* **1B**, 282 (1952).
13. E. CITAKOGLU and J. W. ROSE, Dropwise condensation the effect of surface inclination. *Int. J. Heat Mass Transfer* **12**, 645 (1969).
14. R. E. TOWER and J. W. WESTWATER, Effect of plate inclination on heat transfer during dropwise condensation of steam. *Chem. Engng Prog. Symp. Ser.* **66**(102), 21 (1970).
15. A. UMUR and P. GRIFFITH, Mechanism of dropwise condensation. *J. Heat Transfer* **87**, 275 (1966).
16. J. L. MCCORMICK and J. W. WESTWATER, Drop dynamics and heat transfer during dropwise condensation of water vapor on a horizontal surface. *Chem. Engng Prog. Symp. Ser. No.* 64, **62**, 120 (1966)
17. J. L. MCCORMICK and J. W. WESTWATER, Nucleation sites for dropwise condensation. *Chem. Engng Sci.* **20**, 1021 (1965).
18. A. C. PETERSON and J. W. WESTWATER, Dropwise condensation of ethylene glycol. *Chem. Engng Prog. Symp. Ser.* No. 64, **62**, 135 (1966).
19. R. W. SCHRAGE, *A Theoretical Study of Interphase Mass Transfer*. Columbia University Press, New York (1953).
20. B. MIKIC, On the mechanism of dropwise condensation. *Int. J. Heat Mass Transfer* **12**, 1311 (1969).
21. J. J. LORENZ and B. MIKIC, The effect of thermocapillary flow on heat transfer in dropwise condensation. *J. Heat Transfer* **92**, 46 (1970).
22. N. FATICA and D. L. KATZ, Dropwise condensation. *Chem. Engng Prog.* **45**, 661 (1949).
23. S. SUGAWARA and I. MICHIYOSHI, Dropwise condensation. *Mem. Fac. Engng, Kyoto Univ.* **18**, No. 2 (1956).
24. H. WENZEL, Der Wärmeübergang bei der Tropfenkondensation. *Linde-Ber. Tech. Wiss.* **18**, 44 (1964).
25. E. E. GOSE, A. N. MUCCIARDI and E. BAER, Model for dropwise condensation on randomly distributed sites. *Int. J. Heat Mass Transfer* **10**, 15 (1967).
26. I. TANASAWA and F. TACHIBANA, A synthesis of the total process of dropwise condensation using the method of computer simulation. Proc. Fourth Int. Heat Transfer Conference **6**, paper Cs 1.3 (1970).
27. J. W. WESTWATER, Dropwise condensation. Proc. Fourth Annual Southeastern Seminar on Thermal Sciences, Univ. of Tennessee Space Institute, Tullahoma, Tennessee (1968).
28. E. J. LE FEVRE and J. W. ROSE, A theory of heat transfer by dropwise condensation. Proc. Third Int. Heat Transfer Conference, Am. Inst. Chem. Engrs. New York **2**, 362 (1966).
29. J. F. WELCH and J. W. WESTWATER, Microscopic study of dropwise condensation. International Developments in Heat Transfer, Amer. Soc. Mech. Engrs. New York, **2**, 302 (1961).
30. J. W. ROSE, On the mechanism of dropwise condensation. *Int. J. Heat Mass Transfer* **10**, 755 (1967).
31. I. TANASAWA and J. OCHIAI, Experimental study of dropwise condensation, *Bull. JSME* to be published (1972).
32. L. R. GLICKSMAN and A. W. HUNT, Numerical simulation of dropwise condensation. *Int. J. Heat Mass Transfer* **15**, 2251–2269 (1972).
33. E. J. LE FEVRE and J. W. ROSE, Dropwise condensation. Bicentenary of the James Watt Patent, Proceedings of symposium, Univ. Glasgow, 165 (1969).
34. C. GRAHAM, private communication (1970).

CONDENSATION EN GOUTTES—LA DISTRIBUTION DES TAILLES DES GOUTTES

Résumé—La nature du processus de croissance des gouttes durant la condensation révélée par des films cinématographiques avec fort grossissement (16, 18, 29) est prise pour base d'un modèle simplifié de la séquence des évènements qui se produisent pendant le cycle de croissance (par exemple, l'intervalle de temps entre les balayages successifs de la région superficielle considérée). Le modèle est utilisé pour estimer la distribution moyenne de la taille des gouttes. La distribution théorique est comparée aux mesures (8, 31), à une simulation récente par ordinateur (32) et à une distribution empirique antérieure (28).

TROPFENKONDENSATION—VERTEILUNG DER TROPFENGRÖSSE

Zusammenfassung—Die Natur des Wachstumsprozesses bei der Tropfenkondensation, die in Filmaufnahmen [16, 18, 29] mit starker Vergrösserung sichtbar gemacht ist, wurde als Grundlage für ein vereinfachtes Modell zum Ablauf der Ereignisse während eines Wachstumszyklus (d.h. der Zeit zwischen aufeinanderfolgendem Tropfenablauf auf der betrachteten Fläche) herangezogen. Das Modell dient zur Bestimmung der durchschnittlichen Tropfengrössenverteilung. Die theoretische Verteilung wurde mit Messergebnissen [8, 31], mit einem neueren Rechenmodell [32] und mit einem früheren empirischen Verteilungsgesetz verglichen [28].

КАПЕЛЬНАЯ КОНДЕНСАЦИЯ. РАСПРЕДЕЛЕНИЕ РАЗМЕРОВ КАПЕЛЬ

Аннотация—Механизм процесса роста капель при капельной конденсации, который можно проследить на кинопленке при многократном увеличении [16, 18, 29], лег в основу упрощенной модели последовательных явлений, происходящих во время цикла роста, т.е. промежутка времени между последовательными смывами участка рассматриваемой поверхности. Эта модель используется для расчета среднего распределения размеров капель. Теоретические данные сравниваются с результатами измерений [8, 31], с результатами моделирования на вычислительной машине [32] и с ранее полученными эмпирическими данными [28].